

Cite this: *Chem. Sci.*, 2021, 12, 6442

All publication charges for this article have been paid for by the Royal Society of Chemistry

Electrochemical oxidation of molecular nitrogen to nitric acid – towards a molecular level understanding of the challenges†

Megha Anand,  Christina S. Abraham  and Jens K. Nørskov *

Nitric acid is manufactured by oxidizing ammonia where the ammonia comes from an energy demanding and non-eco-friendly, Haber–Bosch process. Electrochemical oxidation of N_2 to nitric acid using renewable electricity could be a promising alternative to bypass the ammonia route. In this work, we discuss the plausible reaction mechanisms of electrochemical N_2 oxidation (N_2OR) at the molecular level and its competition with the parasitic oxygen evolution reaction (OER). We suggest the design strategies for N_2 oxidation electro-catalysts by first comparing the performance of two catalysts – $TiO_2(110)$ (poor OER catalyst) and $IrO_2(110)$ (good OER catalyst), towards dinitrogen oxidation and then establish trends/scaling relations to correlate OER and N_2OR activities. The challenges associated with electrochemical N_2OR are highlighted.

Received 7th February 2021
Accepted 30th March 2021

DOI: 10.1039/d1sc00752a

rsc.li/chemical-science

Introduction

Nitric acid is an industrially important compound. It is largely used to make nitrate-based fertilizers that are essential for food production from plants.^{1,2} Without the use of fertilizers it would be impossible to feed the 8 billion human population on earth. Nitric acid used as a basis for nitrate fertilizers is manufactured by oxidizing ammonia using the Ostwald process (Fig. 1), and the ammonia used here comes primarily from the Haber–Bosch (HB) process ($N_2 + 3H_2 \rightarrow 2NH_3$).^{3,4} Unfortunately this process requires harsh reaction conditions ($P \sim 150$ atm and $T \sim 700$ K) and it is highly energy intensive, using $\sim 1\%$ of the total global energy consumption. The process has a high carbon-footprint since one of the reactants, H_2 , comes primarily from the steam reforming process where fossil resources react with water to form H_2 and CO_2 (Fig. 1). Approximately 1.9 metric tons of CO_2 is formed per metric ton of NH_3 produced which contributes significantly to the climate change.^{5,6} Hence, it is highly desirable to bypass the ammonia route and develop a direct and sustainable method for N_2 fixation such as alternative routes to nitric acid formation.⁷

Direct oxidation of molecular nitrogen provides a moderately endothermic approach to produce nitrogen oxides and, ultimately, nitric acid (Fig. 1).^{9,10} The reaction is however extremely slow at ambient conditions¹¹ – a good thing in general, since it helps maintain low concentration of NO_x and nitric acid in our ecosystem. Only very high temperatures or plasmas enable reasonable reaction rates.^{12–19}

Electrochemical oxidative fixation of molecular nitrogen (Fig. 1) appears to be a very attractive approach to drive the endothermic reaction at ambient conditions, where the electricity needed can come from the renewable energy sources making the process sustainable. The reaction has an equilibrium potential of 1.32 eV and previous reports suggest that at pHs above 1.3, the formation of nitrate ions is thermodynamically favoured over the parasitic oxygen evolution reaction for a wide range of potentials.⁶

There is a general lack of natural or artificial electro-catalysts for dinitrogen oxidation.²⁰ Recently, a few experimental reports emerged suggesting Pd-decorated MXenes and several oxides as potential electrocatalysts for nitrogen oxidative fixation.^{21–24}

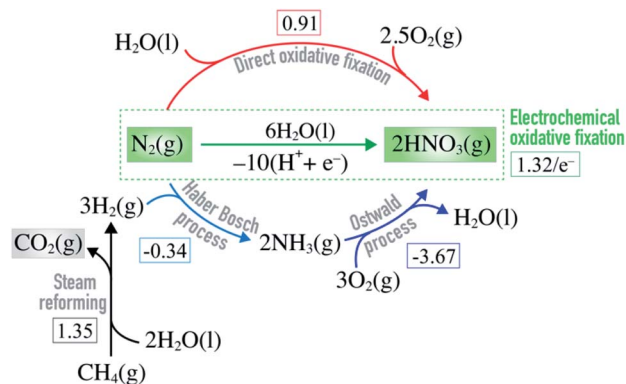


Fig. 1 Equations showing how nitric acid is manufactured on industrial scale by combining steam reforming, Haber–Bosch and Ostwald processes. Direct and electrochemical oxidative N_2 fixation are alternative routes to nitric acid formation. The square brackets contain the free energy of each reaction (in eV) at standard conditions.⁸

Center for Catalysis Theory, Technical University of Denmark, Fysikvej Building 311, 2800 Kongens Lyngby, Denmark. E-mail: jkno@dtu.dk

† Electronic supplementary information (ESI) available. See DOI: 10.1039/d1sc00752a



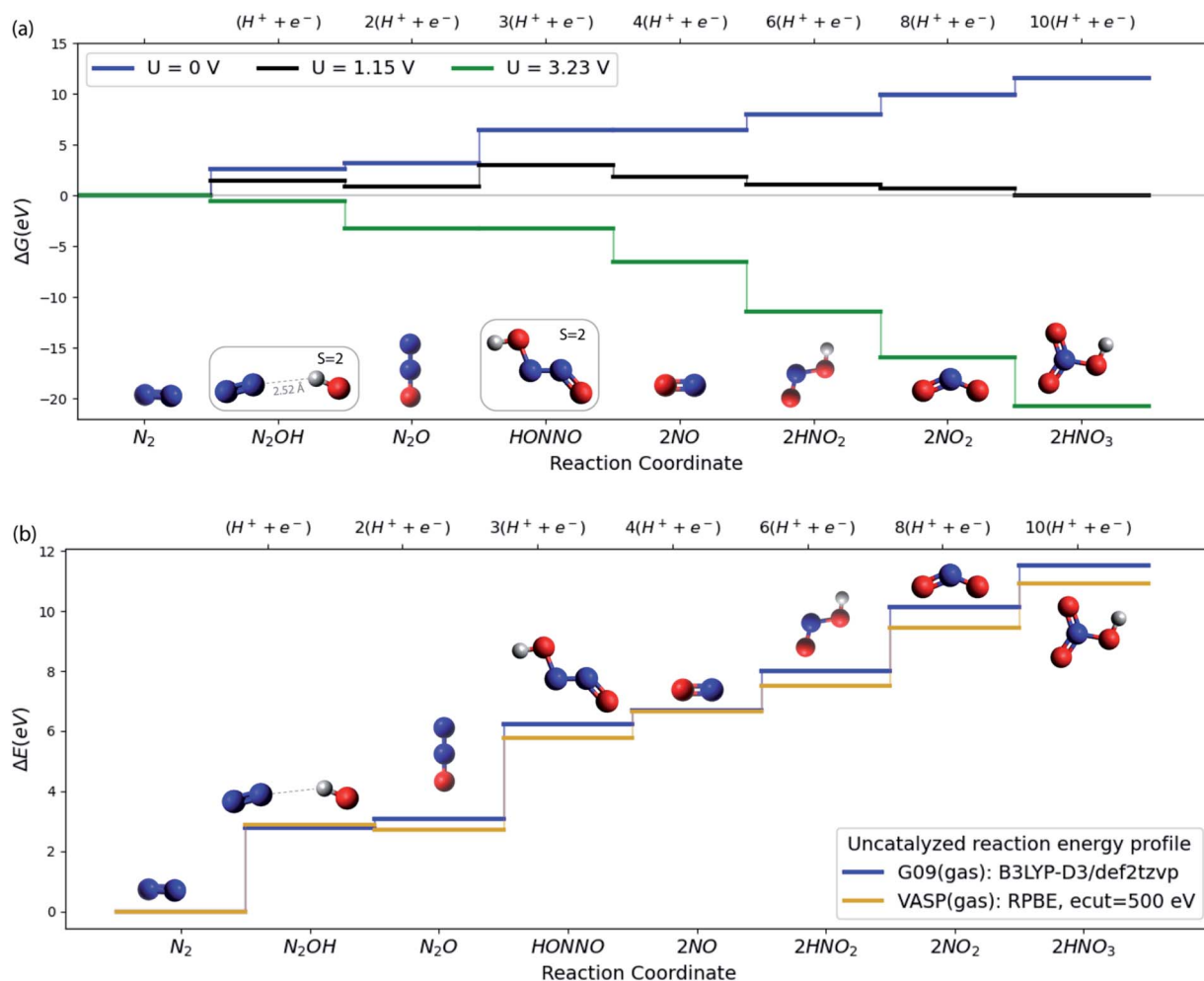


Fig. 2 (a) Free energy plot at SMD(H₂O)/B3LYP-D3/def2tzvp level of theory for N₂ to HNO₃ conversion. All the relative free energies (ΔG) are evaluated with respect to N₂(g), H₂(g) and H₂O(l). The blue, black and green lines refer to the 0, equilibrium (1.15 V) and the limiting (3.23 V) potentials respectively. (b) Comparison of VASP and G09 energies of the N₂OR reaction intermediates in vacuum.

There are numerous reports of oxide photo-catalysts for the N₂ oxidation reaction, prominent among these is TiO₂, but there is also a great deal of controversy in that field, see ref. 10 for a recent thorough review.

In the present paper, we aim at contributing to the theoretical framework for understanding the electrochemical dinitrogen oxidation reaction (N₂OR). The goal is to provide design strategies for N₂OR electro-catalysts both in terms of reaction rates and selectivity towards N₂ oxidation relative to water oxidation (the oxygen evolution reaction, OER). Building on the work of Medford *et al.*,^{25,26} we first discuss the role of a catalyst in terms of stabilization of key intermediates on the basis of a set of density functional theory (DFT) computations. We contrast two catalysts, a good OER catalyst, IrO₂, and a poor OER catalyst, TiO₂. We then identify several possible rate- and selectivity-determining elementary steps and evaluate the corresponding activation energies.

As a starting point, consider in Fig. 2a the free energy diagram for a set of intermediates defining the simplest possible pathway for N₂ oxidation in solution. At the SMD(H₂O)/

B3LYP-D3/def2tzvp level of theory used here (see ESI†/Computational methods section for details), the free energy for this 10-electron electrochemical reaction is 11.5 eV in reasonable agreement with experiment (12.7 eV) when N₂(g), H₂(g) and H₂O(g) are used as the references at standard conditions.⁸ The energetics and the characteristics of the intermediates all agree well with other DFT functionals and experiment as discussed in the ESI.† Fig. 2a illustrates well the difficulty of oxidizing N₂, and the ease of the opposite reaction, reduction of nitrate to form N₂.^{27,28} Applying a positive potential can reduce the thermodynamic barriers for N₂OR, but a very high limiting potential of 3.23 V (*vs.* RHE) is needed in order for all reaction steps to become exergonic.

We now turn to discuss the ways in which a catalyst can facilitate the reaction. We will discuss solid catalysts deposited on an electrode. To this end we need a calculational scheme that can treat semi-infinite solid surfaces. We use VASP^{29–32} with the RPBE exchange–correlation functional,³³ which is known to provide the best treatment of adsorption properties on solid surfaces³⁴ (see ESI†/Computational methods section for



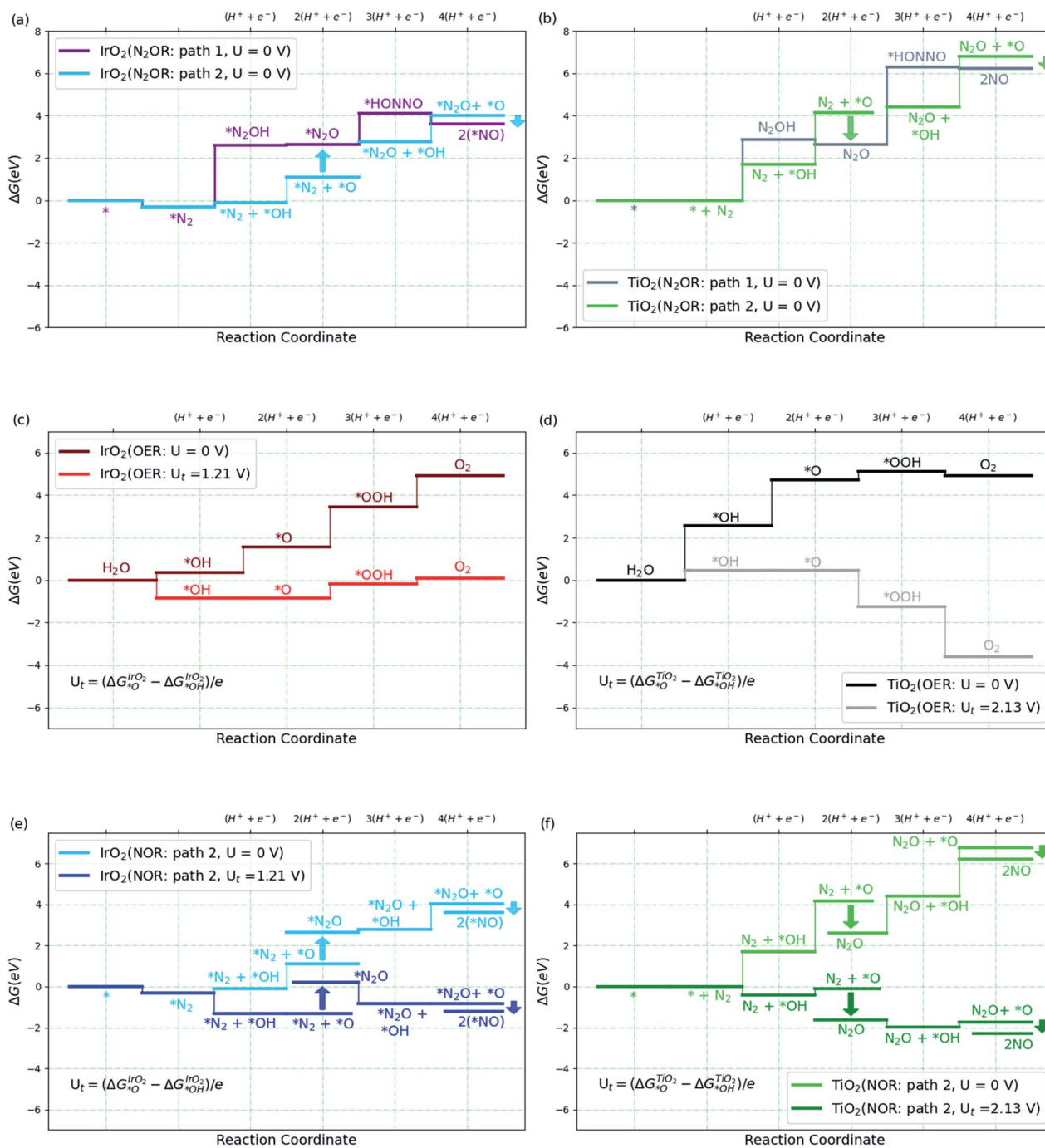


Fig. 3 (a and b) Free energy diagram for N_2 to NO formation through path 1 and path 2 on $\text{IrO}_2(110)$ and $\text{TiO}_2(110)$. (c and d) Free energy diagram for oxygen evolution reaction (OER) on high $\ast\text{O}$ covered $\text{IrO}_2(110)$ and high $\ast\text{OH}$ covered $\text{TiO}_2(110)$ surfaces at two different potentials, U and U_t volts, where U_t is defined in the plot (see ESI† for coverage details). (e and f) Free energy diagram for N_2 to NO formation via path 2 on $\text{IrO}_2(110)$ and $\text{TiO}_2(110)$ at U and U_t volts. The label $2(\ast\text{NO})$ refers to 2 times the $\text{NO}-\text{IrO}_2(110)$ system. All the relative free energies (ΔG) are evaluated with respect to $\text{N}_2(\text{g})$, $\text{H}_2(\text{g})$ and $\text{H}_2\text{O}(\text{l})$.

details). Fig. 2b compares the gas phase energies of reaction intermediates of the uncatalyzed reaction obtained using the RPBE functional in VASP and the B3LYP-D3 functional in Gaussian 09. For the present purposes, the two functionals provide very similar descriptions of the N_2OR process. In the following sections, we base our treatment of the

electrochemical steps on the RPBE functional. We include entropic terms in the harmonic approximation, (see ESI† for details) in the calculation of the free energies but ignore solvation effects at the surface. We have tested this by studying the electrochemical interface between stoichiometric, defect-free (110) rutile TiO_2 and explicitly adsorbed water in order to



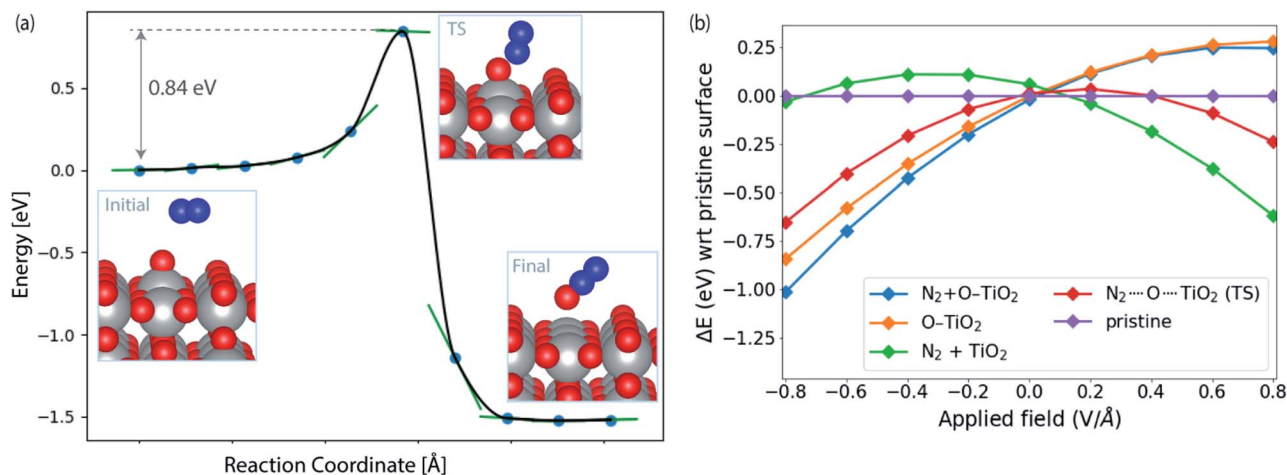


Fig. 4 (a) Reaction pathway and barrier for $*\text{O} + \text{N}_2 \rightarrow \text{N}_2\text{O}$ formation on $\text{TiO}_2(110)$. (b) Influence of applied field on the energies of initial ($\text{N}_2 + \text{O}-\text{TiO}_2$) and transition state ($\text{N}_2 \cdots \text{O} \cdots \text{TiO}_2$) with respect to the pristine slab ($\text{TiO}_2(110)$). The orange and green lines correspond to the initial structure ($\text{N}_2 + \text{O}-\text{TiO}_2$) with N_2 and $*\text{O}$ removed from the surface, respectively. See ESI† for details of field computations.

investigate how the presence of water influences the adsorption of the N_2OR intermediates. We find almost no change in the N_2OR adsorbate binding energy with the inclusion of explicit water molecules (see ESI†/Solvation section for more details).

We then consider the reaction over two transition metal oxide surfaces, IrO_2 and TiO_2 , both in the rutile structure and in both cases, we consider the (110) facets. Both materials are stable under highly oxidizing conditions, for IrO_2 at least up to potentials of interest for the oxygen evolution reaction.^{9,35–38} Here we focus on the path to producing NO , since the steps following that are relatively facile even at the equilibrium potential, as shown in Fig. 2a. Fig. 3a and b show the free energy diagram for two pathways for the two surfaces. Path 1 is the one we studied in solution (Fig. 2a), while the new path 2, starts with water oxidation to form adsorbed OH as first discussed by Medford and co-workers.²⁶ The formation of adsorbed OH is less endergonic than the first oxidation step of N_2 to form adsorbed N_2OH for both surfaces. We therefore concentrate on path 2 in the following sections.

Adsorbed OH (or $*\text{OH}$) can react with N_2 involving a proton and electron transfer to form N_2O ($*\text{OH} + \text{N}_2 \rightarrow \text{N}_2\text{O} + \text{H}^+ + \text{e}^-$). Alternatively, $*\text{OH}$ can be oxidized further to form adsorbed O , which can react in two ways. It can form O_2 by direct recombination or react with water in an electrochemical process to form adsorbed OOH and, after another electron and proton transfer, O_2 , Fig. 3c and d. This is the usual oxygen evolution reaction. Alternatively, the adsorbed O can react with N_2 in a non-electrochemical process $*\text{O} + \text{N}_2 \rightarrow *\text{N}_2\text{O}$, and further, $*\text{O} + \text{N}_2\text{O} \rightarrow 2*\text{NO}$ ($=*\text{N}_2\text{O}_2$) (Fig. 3e and f). It can be seen that, as expected, OER is much more facile than N_2OR for IrO_2 . Indeed, for IrO_2 , $*\text{N}_2\text{O}$ is considerably less stable than $*\text{O} + *\text{N}_2$ making the N_2OR reaction very slow, while OER becomes facile thermochemically at potentials above 1.5 V. On TiO_2 , on the other hand, the adsorbed O is so unstable, that N_2O formation is highly exergonic. We therefore discuss TiO_2 in more detail below.

Most of the reaction steps in Fig. 3e and f involve proton transfers from oxygen to water (in acidic conditions). Such barriers have been found to be very small, of the order 0.2 eV, in studies of water oxidation.³⁹ We expect the highest barriers to be associated with the activation of N_2 . For the N_2OR path 2, there are two possible rate determining steps to form N_2O , the electrochemical pathway, $*\text{OH} + \text{N}_2 \rightarrow \text{N}_2\text{O} + \text{H}^+ + \text{e}^-$ or the purely chemical pathway, $*\text{O} + \text{N}_2 \rightarrow \text{N}_2\text{O}$. In the following, we explore the chemical pathway, including the next chemical step, $*\text{O} + \text{N}_2\text{O} \rightarrow \text{N}_2\text{O}_2 \rightarrow 2*\text{NO}$.

Fig. 4a shows the calculated activation energy for the reaction $*\text{O} + \text{N}_2 \rightarrow \text{N}_2\text{O}$ over a $\text{TiO}_2(110)$ surface. A value of 0.84 eV is found at this level of theory. Outside an electrode surface we need to include electric field effects. It can be seen in Fig. 3f that we need to apply a potential of $U_t = (\Delta G_{\text{O}} - \Delta G_{\text{OH}})/e$ in order for adsorbed O to become thermodynamically stable at the surface. For TiO_2 , this value is $U_t = 2.13$ V. If we assume a width of 3 Å for the Helmholtz layer outside the electrode,⁴⁰ this corresponds to a field strength of the order of $E \sim U_t/d \sim 0.7 \text{ V } \text{Å}^{-1}$, depending

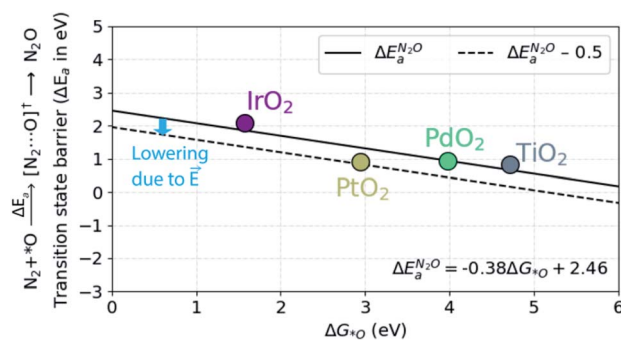


Fig. 5 Scaling relationship between ΔG_{O} and the barrier (ΔE_{a}) for the N_2O formation. The dotted line includes the 0.5 eV lowering of the barrier due to the local electric field that exists in the electric double-layer at the electrode–electrolyte interface in electrochemical reactions.

on the value of the potential of zero charge of the system. In Fig. 4b we show the energy of adsorbed O and the transition state of N₂O formation as a function of field strength outside a TiO₂(110) surface. Clearly *O is strongly destabilized while the transition state is stabilized at positive fields. For TiO₂, the net effect is a reduction of the activation energy of the order 0.5 eV. Finally, in order to evaluate the activation free energy, we need to include the loss of gas phase entropy of N₂ during the reaction. This would add an energy of the order of 0.6 eV to the free energy barrier for the reaction (see ESI† for more details). The net free energy barrier is thus of the order 1 eV according to this very rough estimate.

An activation free energy of the order 1 eV should give a measurable N₂OR rate unless the selectivity is low. Based on the model developed in ref. 39 to estimate the activation energy for OER over TiO₂, the activation energy for oxygen evolution is considerably low. Even given the crudeness of the estimate of the free energy barrier for N₂OR, this result strongly suggests that N₂OR through the direct chemical reaction of N₂ and N₂O with adsorbed O is difficult over TiO₂. We cannot rule out that the alternative electrochemical process, *OH + N₂ → N₂O + H⁺ + e⁻, will work. That is beyond the present work. We find similar activation barrier of 0.77 eV for the N₂O₂ formation (*O + N₂O → N₂O₂).

In order to understand the trends in the chemical N₂O formation barrier we show in Fig. 5 the variation in the activation energy to form N₂O with the O adsorption energy including additional oxide surface models. There is a strong linear scaling such that a weaker O adsorption bond gives a lower activation energy. A more facile N₂OR process would therefore require a catalyst binding O even weaker than TiO₂. The problem is that such a material would still have low activation energy for OER according to the model in ref. 39.

A more promising strategy towards a high selectivity may be to impede the electrochemical oxygen evolution (OER) step relative to the chemical N₂OR steps. This can be accomplished by limiting the access to either proton acceptors or electron acceptors (holes). Limited access to proton acceptors can be accomplished by using a non-aqueous solvent with few proton acceptors. A similar strategy has already been used successfully to increase the selectivity of electrochemical N₂ reduction (where the parasitic reaction is hydrogen evolution).^{41–44} Limited access to holes can for instance be achieved by limiting conductivity to the surface. For TiO₂ this could be achieved by controlling the thickness of a non-conducting TiO₂ film on the electrode surface.⁴⁵ Limited access to holes could be what is achieved in photochemical N₂OR. We note that any lowering of the electrochemical rates will of course lower the overall rate since the first N₂OR steps are electrochemical.

Conclusions

In conclusion, we provide a molecular level understanding of the challenges associated with the electrochemical nitrogen oxidation reaction. We analyse the possibility of N₂OR on an excellent OER catalyst, IrO₂(110) and a poor OER catalyst TiO₂(110). Obviously OER supersedes N₂OR on IrO₂ and TiO₂

turns out to be a borderline N₂OR catalyst. We suggest ways to suppress OER in order to promote N₂OR on oxide surfaces.

Author contributions

J. K. N. and M. A. conceptualised the paper. M. A. performed all the computations except the aqueous stability computations which were done by C. S. A. All authors contributed towards writing the manuscript.

Conflicts of interest

There are no conflicts to declare.

Acknowledgements

This work was supported by the Toyota Research Institute and V-Sustain: The VILLUM Centre for the Science of Sustainable Fuels and Chemicals (9455) from VILLUM FONDEN.

Notes and references

- 1 J. M. Modak, Haber Process for Ammonia Synthesis, *Resonance*, 2002, 69–77.
- 2 T. Kandemir, M. E. Schuster, A. Senyshyn, M. Behrens and R. Schlögl, The Haber–Bosch Process Revisited: On the Real Structure and Stability of “Ammonia Iron” under Working Conditions, *Angew. Chem., Int. Ed.*, 2013, **52**, 12723–12726.
- 3 K. Wang, D. Smith and Y. Zheng, Electron-driven heterogeneous catalytic synthesis of ammonia: current states and perspective, *Carbon Resour. Convers.*, 2018, **1**, 2–31.
- 4 A. Valera-Medina, H. Xiao, M. Owen-Jones, W. I. David and P. J. Bowen, Ammonia for power, *Prog. Energy Combust. Sci.*, 2018, **69**, 63–102.
- 5 R. Schlögl, Catalytic synthesis of ammonia – a “never-ending story”?, *Angew. Chem., Int. Ed.*, 2003, **42**, 2004–2008.
- 6 J. G. Chen, *et al.* Beyond fossil fuel-driven nitrogen transformations, *Science*, 2018, 360.
- 7 J. Baltrusaitis, Sustainable Ammonia Production, *ACS Sustainable Chem. Eng.*, 2017, **5**, 9527.
- 8 D. D. Wagman, W. H. Evans, V. B. Parker, R. H. Schumm, I. Halow, S. M. Bailey, K. L. Churney and R. L. Nuttall, The NBS tables of chemical thermodynamic properties: selected values for inorganic and C1 and C2 organic substances in SI units, *J. Phys. Chem. Ref. Data*, 1982, 111–518.
- 9 M. Pourbaix, *Atlas of electrochemical equilibria in aqueous solutions*, Tex: National Association of Corrosion Engineers, Houston, Texas, 1974, p. 500.
- 10 A. J. Medford and M. C. Hatzell, Photon-driven nitrogen fixation: current progress, thermodynamic considerations, and future outlook, *ACS Catal.*, 2017, **7**, 2624–2643.
- 11 G. Charlot, *L'analyse qualitative et les réactions en solution*, 1957, pp. 315–321.



- 12 Y. Wang, A. W. Desilva, G. C. Goldenbaum and R. R. Dickerson, Nitric oxide production by simulated lightning – dependence on current energy and pressure, *J. Geophys. Res.*, 1998, **103**, 19149–19159.
- 13 B. S. Patil, Q. Wang, V. Hessel and J. Lang, Plasma N₂-fixation: 1900–2014, *Catal. Today*, 2015, **256**, 49–66.
- 14 N. Cherkasov, A. O. Ibhadon and P. Fitzpatrick, A review of the existing and alternative methods for greener nitrogen fixation, *Chem. Eng. Process.*, 2015, **90**, 24–33.
- 15 X. Fan, S. Kang, J. Li and T. Zhu, Formation of nitrogen oxides (N₂O, NO, and NO₂) in typical plasma and plasma-catalytic processes for air pollution control, *Water, Air, Soil Pollut.*, 2018, **229**, 351–363.
- 16 Y. He, Z. Chen, Z. Li, G. Niu and J. Tang, Non-thermal plasma fixing of nitrogen into nitrate: solution for renewable electricity storage?, *Front. Optoelectron.*, 2018, **11**, 92–96.
- 17 S. Li, J. A. M. Jimenez, V. Hessel and F. Gallucci, Recent progress of plasma-assisted nitrogen fixation research: a review, *Processes*, 2018, **6**, 248–273.
- 18 P. Lamichhane, R. Paneru, L. N. Nguyen, J. S. Lim, P. Bhartiya, B. C. Adhikari, S. Mumtaz and E. H. Choi, Plasma-assisted nitrogen fixation in water with various metals, *React. Chem. Eng.*, 2020, **5**, 2053–2057.
- 19 Z. Liu, Y. Tian, G. Niu, X. Wang and Y. Duan, Direct Oxidative Nitrogen Fixation from Air and H₂O by a Water Falling Film Dielectric Barrier Discharge Reactor at Ambient Pressure and Temperature, *ChemSusChem*, 2021, **14**, 1507–1511.
- 20 Y. Wang, Y. Yu, R. Jia, C. Zhang and B. Zhang, Electrochemical synthesis of nitric acid from air and ammonia through waste utilization, *Natl. Sci. Rev.*, 2019, **6**, 730–738.
- 21 W. Fang, C. Du, M. Kuang, M. Chen, W. Huang, H. Ren, J. Xu, A. Feldhoff and Q. Yan, Boosting efficient ambient nitrogen oxidation by a well-dispersed Pd on MXene electrocatalyst, *Chem. Commun.*, 2020, **56**, 5779–5782.
- 22 C. Dai, Y. Sun, G. Chen, A. C. Fisher and Z. J. Xu, Electrochemical Oxidation of Nitrogen towards Direct Nitrate Production on Spinel Oxides, *Angew. Chem.*, 2020, **59**, 9418–9422.
- 23 M. Kuang, *et al.* Efficient Nitrate Synthesis *via* Ambient Nitrogen Oxidation with Ru-Doped TiO₂/RuO₂ Electrocatalysts, *Adv. Mater.*, 2020, 2002189–2002196.
- 24 S. Han, C. Wang, Y. Wang, Y. Yu and B. Zhang, Electrosynthesis of nitrate *via* the oxidation of nitrogen on tensile strained palladium porous nanosheets, *Angew. Chem., Int. Ed.*, 2021, **133**, 1–6.
- 25 B. M. Comer, Y.-H. Liu, M. B. Dixit, K. B. Hatzell, Y. Ye, E. J. Crumlin, M. C. Hatzell and A. J. Medford, The Role of Adventitious Carbon in Photo-Catalytic Nitrogen Fixation by Titania, *J. Am. Chem. Soc.*, 2018, **140**, 15157–15160.
- 26 B. M. Comer and A. J. Medford, Analysis of Photocatalytic Nitrogen Fixation on Rutile TiO₂(110), *ACS Sustainable Chem. Eng.*, 2018, **6**, 4648–4660.
- 27 V. Rosca, M. Duca, M. T. De Groot and M. T. M. Koper, Nitrogen Cycle Electrocatalysis, *Chem. Rev.*, 2009, **109**, 2209–2244.
- 28 M. Duca and M. T. M. Koper, Powering denitrification: the perspectives of electrocatalytic nitrate reduction, *Energy Environ. Sci.*, 2012, **5**, 9726–9742.
- 29 J. Hafner and G. Kresse, *Ab Initio* Molecular Dynamics for Liquid Metals, *Phys. Rev. B: Condens. Matter Mater. Phys.*, 1993, **47**, 558–561.
- 30 J. Hafner and G. Kresse, *Ab Initio* Molecular-Dynamics Simulation of the Liquid-Metal-Amorphous-Semiconductor Transition in Germanium, *Phys. Rev. B: Condens. Matter Mater. Phys.*, 1994, **49**, 14251–14269.
- 31 G. Kresse and J. Furthmüller, Efficiency of *Ab Initio* Total Energy Calculations for Metals and Semiconductors Using a Plane-Wave Basis Set, *Comput. Mater. Sci.*, 1996, **6**, 15–50.
- 32 G. Kresse and J. Furthmüller, Efficient Iterative Schemes for *Ab Initio* Total-Energy Calculations Using a Plane-Wave Basis Set, *Phys. Rev. B: Condens. Matter Mater. Phys.*, 1996, **54**, 11169–11186.
- 33 B. Hammer, L. Hansen and J. K. Nørskov, Improved adsorption energetics within density functional theory using revised Perdew–Burke–Ernzerhof functionals, *Phys. Rev. B: Condens. Matter Mater. Phys.*, 1999, **59**, 7413–7421.
- 34 J. Wellendorff, K. T. Lundgaard, A. Møgelhøj, V. Petzold, D. D. Landis, J. K. Nørskov, T. Bligaard and K. W. Jacobsen, Density functionals for surface science: exchange–correlation model development with Bayesian error estimation, *Phys. Rev. B: Condens. Matter Mater. Phys.*, 2012, **85**, 235149–235172.
- 35 D.-S. Kong and J.-X. Wu, An Electrochemical Study on the Anodic Oxygen Evolution on Oxide Film Covered Titanium, *J. Electrochem. Soc.*, 2008, **155**, C32.
- 36 S. Cherevko, S. Geiger, O. Kasian, N. Kulyk, J. P. Grote, A. Savan, B. R. Shrestha, S. Merzlikin, B. Breitbach, A. Ludwig and K. J. Mayrhofer, Oxygen and hydrogen evolution reactions on Ru, RuO₂, Ir, and IrO₂ thin film electrodes in acidic and alkaline electrolytes: a comparative study on activity and stability, *Catal. Today*, 2016, **262**, 170–180.
- 37 S. Geiger, O. Kasian, M. Ledendecker, E. Pizzutilo, A. M. Mingers, W. T. Fu, O. Diaz-Morales, Z. Li, T. Oellers, L. Fruchter, A. Ludwig, K. J. Mayrhofer, M. T. Koper and S. Cherevko, The stability number as a metric for electrocatalyst stability benchmarking, *Nat. Catal.*, 2018, **1**, 508–515.
- 38 Z. Wang, X. Guo, J. Montoya and J. K. Nørskov, Predicting aqueous stability of solid with computed Pourbaix diagram using SCAN functional, *npj Comput. Mater.*, 2020, **160**, 1–7.
- 39 C. F. Dickens, C. Kirk and J. K. Nørskov, Insights into the electrochemical oxygen evolution reaction with *ab initio* calculations and microkinetic modeling: beyond the limiting potential volcano, *J. Phys. Chem. C*, 2019, **123**, 18960–18977.
- 40 G. S. Karlberg, J. Rossmeisl and J. K. Nørskov, Estimations of electric field effects on the oxygen reduction reaction based on the density functional theory, *Phys. Chem. Chem. Phys.*, 2007, **9**, 5158.



- 41 A. Tsuneto, A. Kudo and T. Sakata, Efficient Electrochemical Reduction of N_2 to NH_3 catalyzed by Lithium, *Chem. Lett.*, 1993, 851–854.
- 42 A. Tsuneto, A. Kudo and T. Sakata, Lithium-mediated electrochemical reduction of high pressure N_2 to NH_3 , *J. Electroanal. Chem.*, 1994, **367**, 851–854.
- 43 S. Z. Andersen, M. J. Statt, V. J. Bukas, S. G. Shapel, J. B. Pedersen, K. Kreml, M. Saccoccio, D. Chakraborty, J. Kibsgaard, P. C. K. Vesborg, J. Nørskov and I. Chorkendorff, Increasing stability, efficiency, and fundamental understanding of lithium-mediated electrochemical nitrogen reduction, *Energy Environ. Sci.*, 2020, **13**, 4291–4300.
- 44 N. Lazouski, M. Chung, K. Williams, M. L. Gala and K. Manthiram, Non-aqueous gas diffusion electrodes for rapid ammonia synthesis from nitrogen and water-splitting derived hydrogen, *Nat. Catal.*, 2020, **3**, 463–469.
- 45 V. Viswanathan, K. L. Pickrahn, A. C. Luntz, S. F. Bent and J. K. Nørskov, Nanoscale limitations in metal oxide electrocatalysts for oxygen evolution, *Nano Lett.*, 2014, **14**, 5853–5857.

